Electronic Supplementary Material (ESI) for Nanoscale.

Supporting Information

Hierarchical S-modified Cu porous nanoflakes for efficient CO_2 electroreduction to formate

Li-Xia Liu, Xiang Li, Yanming Cai, Huitong Du, Fuqiang Liu, Jian-Rong Zhang, Jiaju Fu* and Wenlei Zhu*

State Key Laboratory of Pollution Control and Resource Reuse, State Key Laboratory of Analytical Chemistry for Life Science, the Frontiers Science Center for Critical Earth Material Cycling, School of the Environment, School of Chemistry and Chemical Engineering, Nanjing University, Nanjing 210023, People's Republic of China.

*Corresponding authors.

E-mail addresses: fujiaju@iccas.ac.cn; wenleizhu@nju.edu.cn

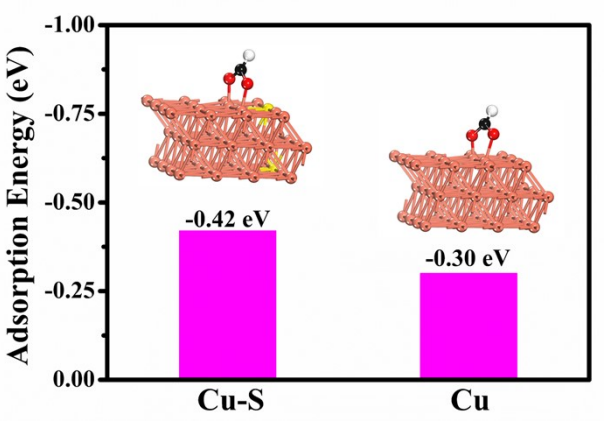

Fig. S1 The calculated adsorption energy of *OCHO on the Cu-S (111) plane and Cu (111) plane.

The more negative adsorption energy of *OCHO was observed for Cu-S relative to Cu, suggesting that *OCHO was favorable to be adducted onto the surface of Cu-S than onto the surface of Cu. As a result, the formate production from CO_2 reduction reaction was predicated to occur easier on the Cu-S surface than on the Cu surface.[1,2]

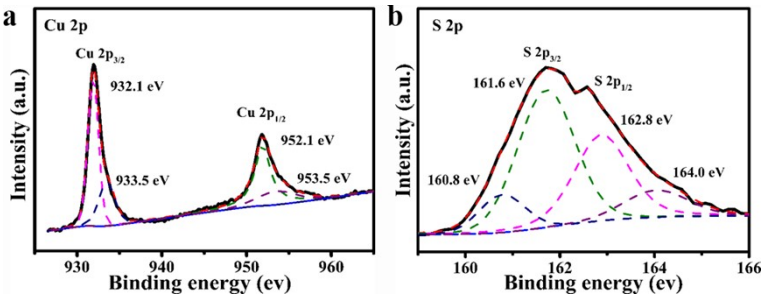

Fig. S2 High-resolution XPS spectra of (a) Cu 2p and (b) S 2p for the as-prepared CuS precursor.

The Cu 2p peaks of the materials showed two strong peaks of Cu $2p_{3/2}$ and Cu $2p_{1/2}$ at 932.1/952.1 eV, which was assigned to the CuS phase.[3] In addition, the small shoulder peaks at 933.5 and 953.5 eV originated from the CuO on the sample surface.[4] The high-resolution XPS spectrum of S 2p showed two main peaks at 161.6 and 162.8 eV, corresponding to the S $2p_{3/2}$ and S $2p_{1/2}$, respectively. Besides, two side peaks at 160.8 eV and 164.0 were related to sulfides (S^{2-}) and disulfide (S_2^{2-}).[3] Via the quantification analysis of Cu and S peak areas, the atomic ratio of Cu : S was estimated to be 1: 1.1, closely matching the stoichiometry of CuS.[5]

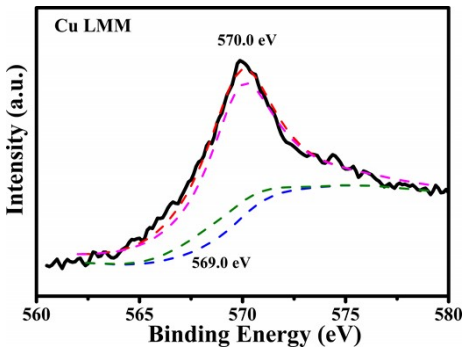

Fig. S3 The Cu LMM spectra of the prepared hierarchical Cu-S NFs.

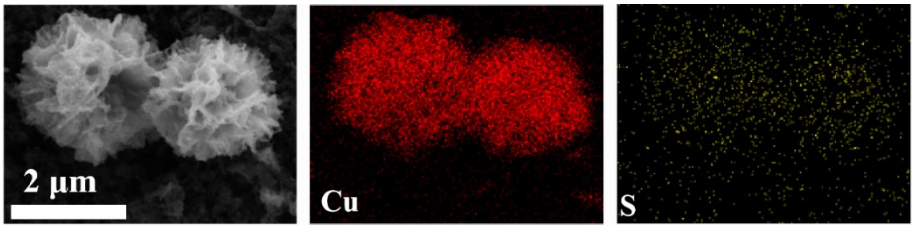

Fig. S4 The SEM images of the as-prepared hierarchical Cu-S NFs and their corresponding element mapping. To avoid interfering with the results of the experiment, the Nafion binder was not added to the prepared sample for element mapping.

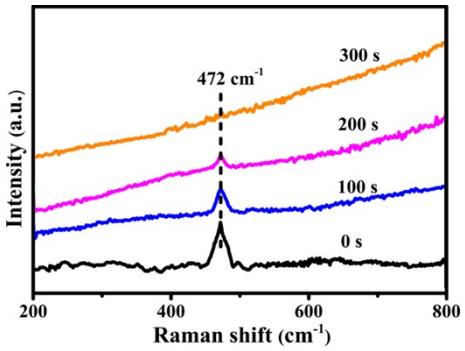

Fig. S5 In situ Raman spectra of hierarchical CuS NFs at −0.60 V vs. RHE with different reduction times.

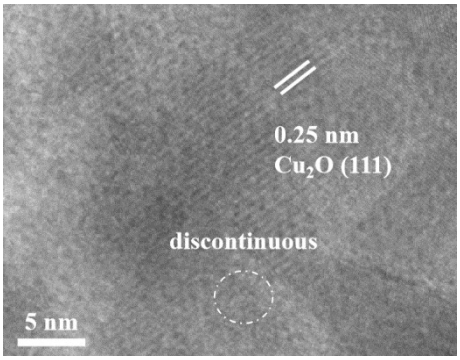

Fig. S6 HRTEM image of the Cu-S NFs.

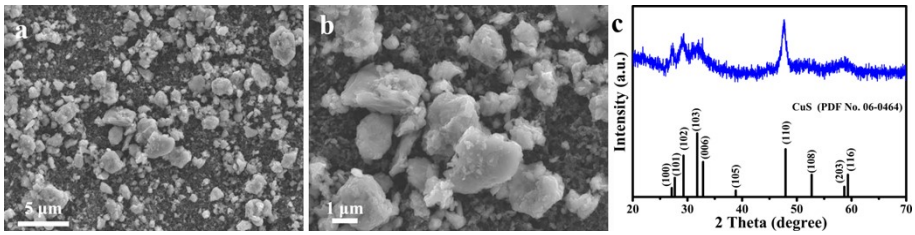

Fig. S7 XRD patterns (a) and SEM images (b, c) of CuS microparticles.

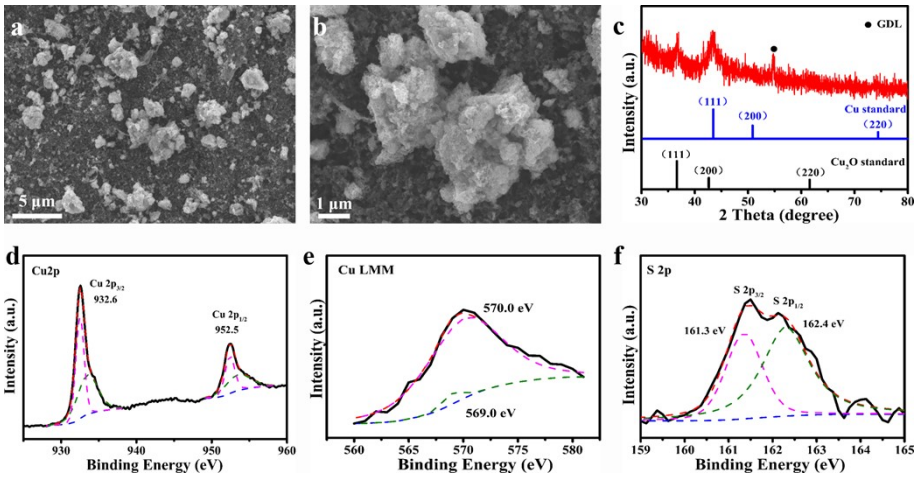

Fig. S8 XRD patterns (a) and SEM images (b, c) of the Cu-S microparticles and their XPS spectra of Cu 2p (d), Cu LMM (e), and S 2p (f).

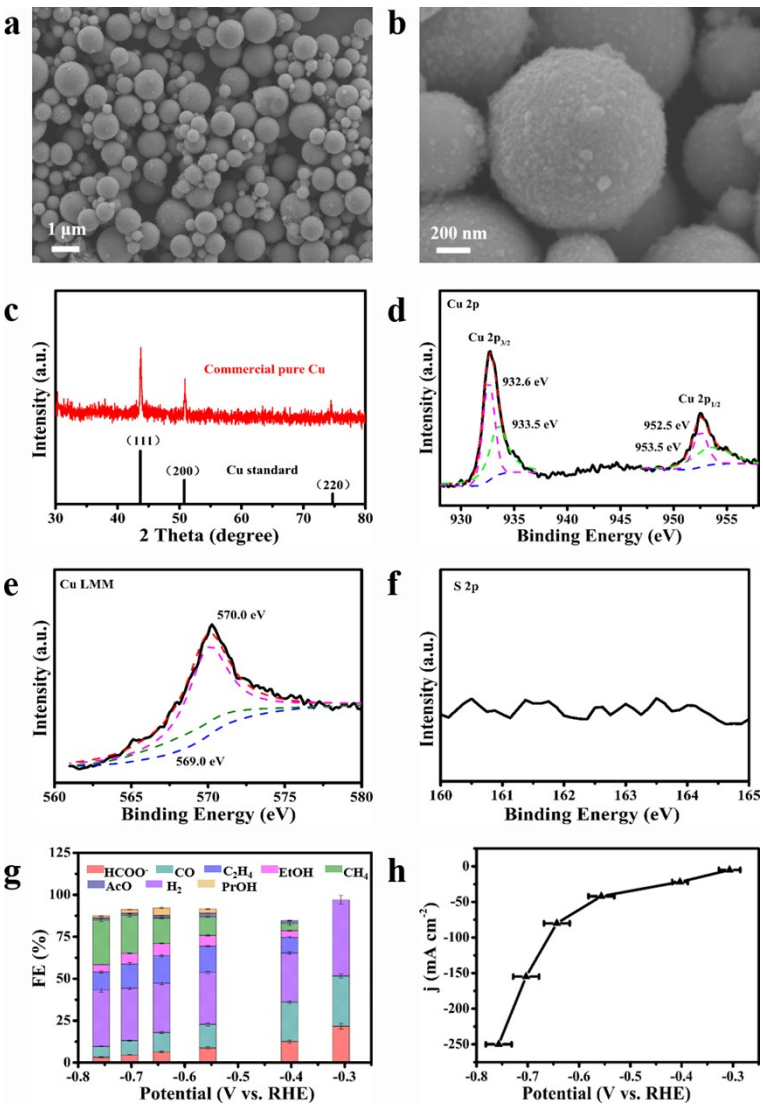

Fig. S9 The characterization of commercial pure Cu catalysts: SEM images (a,b); XRD pattern (c); High-resolution XPS spectra of Cu 2p (d), Cu LMM (e), and S 2p (f). CO_2RR performance of the commercial pure Cu catalysts: Faradaic efficiency of products (g) and the total current density versus the applied potentials.

The XRD results in Fig. S8 showed that the commercial pure Cu catalysts were metallic Cu phase. And the high-resolution XPS results of Cu 2p and the Cu LMM results illustrated that the sample surface was mainly Cu^{+} (932.6 eV, 952.5 eV, 570. 0 eV), with a small number of Cu^{2+} (933.5 eV, 953.5 eV, 569.0 eV).[4,6] In addition, the S 2p XPS spectra proved that there was no S element on the pure Cu surface.

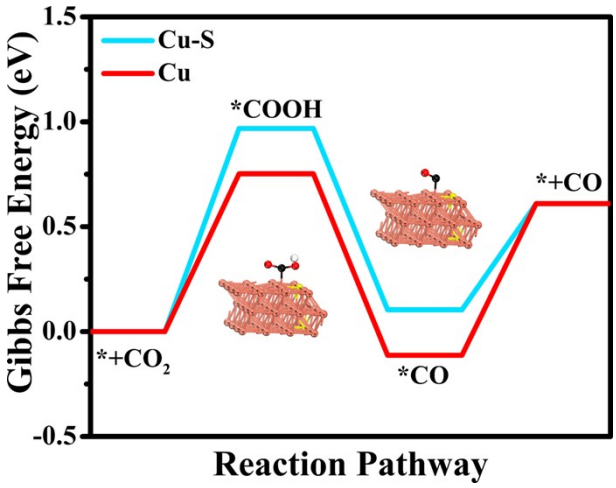

Fig. S10 The DFT calculated free energy of CO_2 reduction to CO on the Cu-S (111) plane and Cu (111) plane.

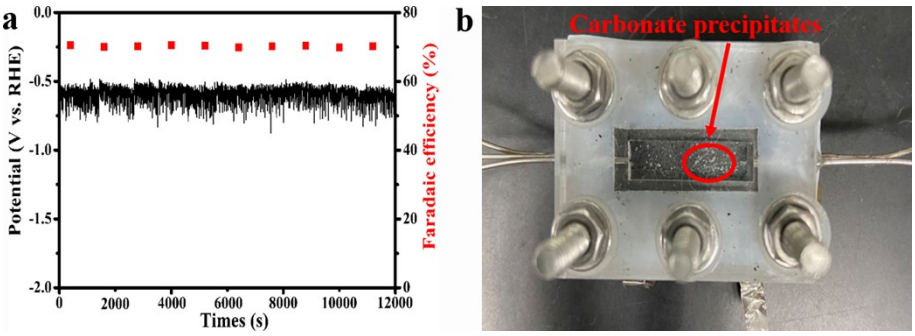

Fig. S11 (a) The potential curves and formate FE at a fixed current density of 200 mA cm^{-2}. (b) Image of the macroporous layer side of the GDL electrode showing carbonate precipitation (circled in red) after continuous operation for 12000 s.

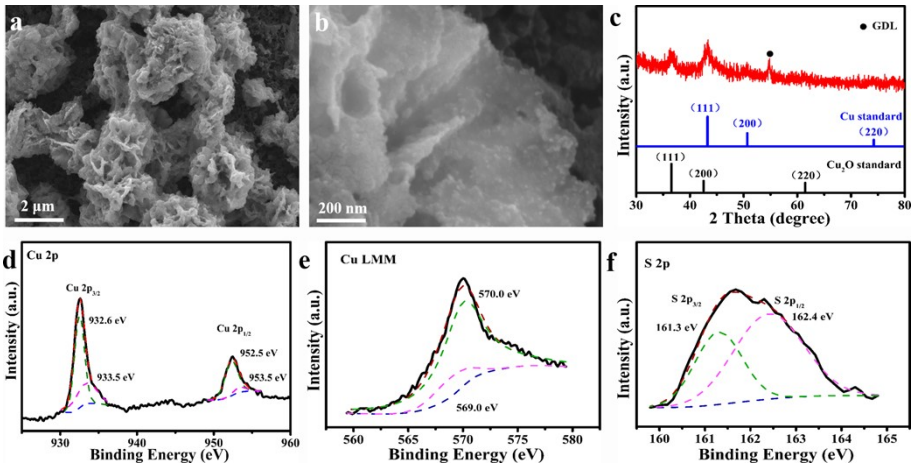

Fig. S12 SEM images (a, b), XRD pattern (c), and XPS spectra (d, e, f) of the hierarchical Cu-S NF catalysts after the stability measurement at 200 mA cm^{-2} current density for 12000 s.

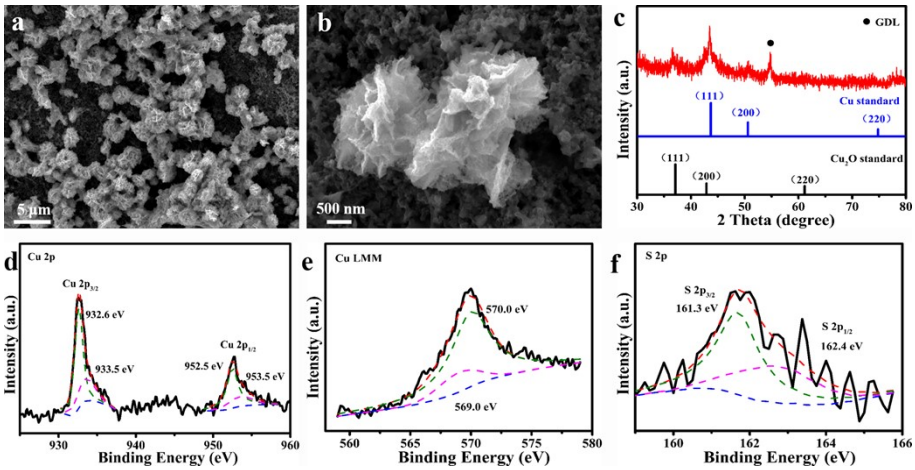

Fig. S13 SEM images (a, b), XRD pattern (c), and XPS spectra (d, e, f) of the hierarchical Cu-S NF catalysts after the stability measurement at 200 mA cm^{-2} current density for 12 h.

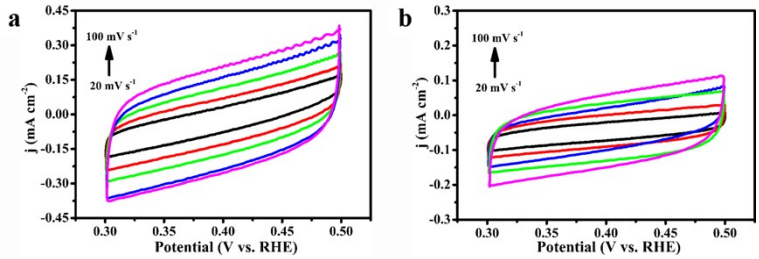

Fig. S14 Cyclic voltammetry curves of hierarchical Cu-S NF electrode (a) and Cu-S MP electrode (b).

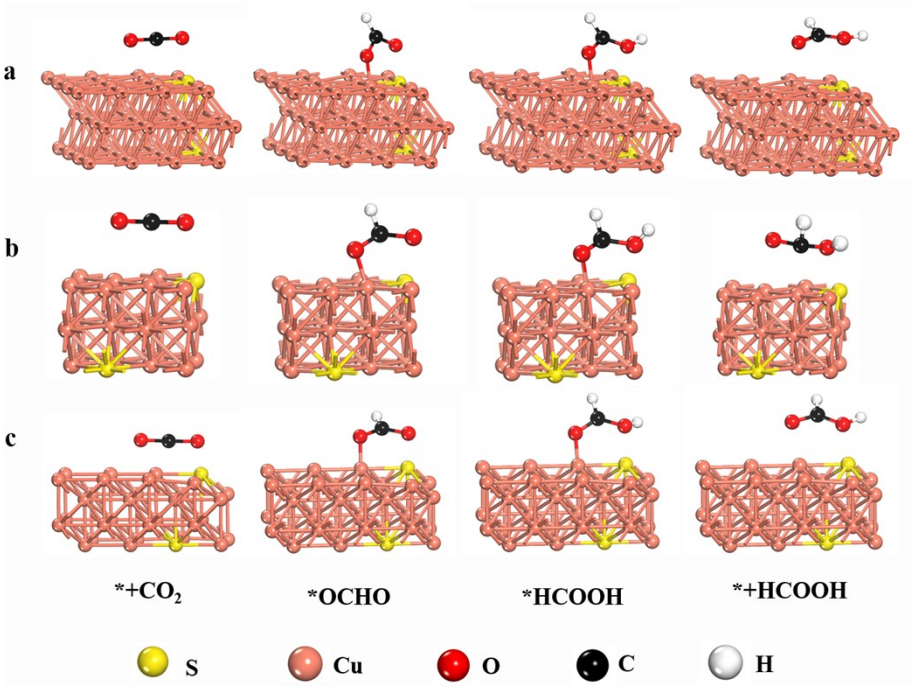

Fig. S15 The DFT-optimized intermediate species along with the reduction reaction of CO_2 to formate on the plane sites of Cu-S: (a) (111) face, (b) (200) face, and (c) (220) face.

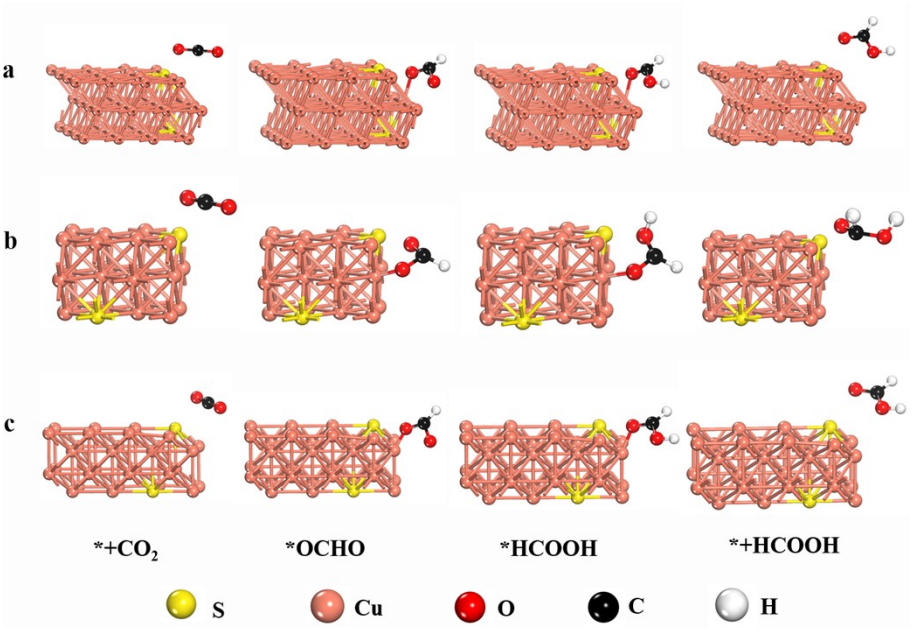

Fig. S16 The DFT-optimized intermediate species along with the reduction reaction of CO_2 to formate on the edge sites of Cu-S: (a) (111) face, (b) (200) face, and (c) (220) face.

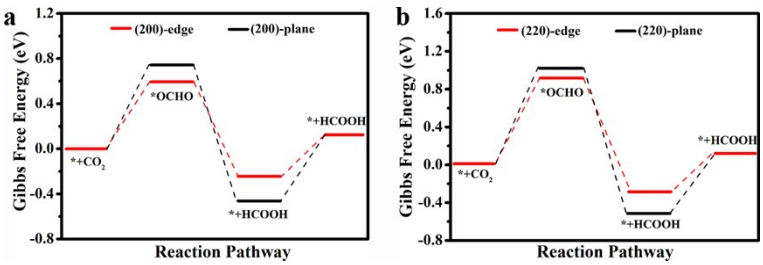

Fig. S17 DFT-calculated *ΔG* on the (200) plane (a) and (220) plane (b) of the Cu-S in the reaction pathway of CO_2 reduction to formate.

Supplementary Tables

Table S1. Performance comparison of hierarchical Cu-S NFs for electrocatalytic CO_2RR towards formate production with a few best electrocatalysts in the literature.

Electrocatalyst	Electrolyte	Potential (V vs. RHE)	$FE_{formate}$ (%)	Formate current density (mA cm^{-2})	Ref.
Hierarchical Cu-S nanoflakes on GDL	1 M KOH	–0.71	89.8	404.1	**This work**
		–0.75	71.5	429.0	
Cu-2.0C on Cu foil	0.1 M $NaHCO_3$	–0.90	87%	19.1	7
S-modified Cu nanoparticles on GDL	0.1 M $KHCO_3$	–0.80	80	~12.0	8
CuSx	0.1 M $KHCO_3$	–0.90	75	6.75	9
Sulfur-doped Cu on Cu disks	0.1 M $KHCO_3$	-0.9	< 60%	13.9	10
SnO_2 nanosheets	1 M $KHCO_3$	–1.13	94.2	471	11
hydrogen-incorporated SnS_2	0.1 M $KHCO_3$	–0.90	87%	24.4	12
Mesoporous SnO_2 nanosheet	0.1 M $KHCO_3$	–0.99	87.0	39.2	13
Bi_2O_3@C-800	1 M KOH	–1.1	93	208	14
Bi NSs	0.1 M $KHCO_3$	–1.1	92	15	15
Dendritic Bi	0.5 M $KHCO_3$	–0.82	92	87.4	16
$BiVO_4$ derived Bi nanoflakes	1 M $KHCO_3$	-1.0	97.4	102.7	17

Table S2. The atomic percent of the S element in Cu-S materials was calculated from the XPS results.

Materials	Hierarchical Cu-S NFs	Cu-S NPs	Hierarchical Cu-S NFs after stability test	
			12000 s	12 h
The atomic percent of the S element	1.85	1.82	1.71	1.68

Table S3. The DFT calculated the *ΔG* value of different species on the edge sites and plane sites of Cu-S materials for (111) face, (200) face, and (220) face.

	Edge sites			Plane sites		
	(111) face	(200) face	(220) face	(111) face	(200) face	(220) face
*+CO_2	0	0	0	0	0	0
*OCHO	0.28227	0.59134	0.91598	0.46038	0.74532	1.0151
*HCOOH	-0.19728	-0.24712	-0.28226	-0.42758	-0.46104	-0.50773
*+HCOOH	0.12477	0.12477	0.12477	0.12477	0.12477	0.12477

Supplementary References

1. Z. Chen, K. Mou, X. Wang and L. Liu, *Angew. Chem. Int. Ed.* 2018, **130**, 12792-12796.

2. Z. Chen, X. Zhang, M. Jiao, K. Mou, X. Zhang and L. Liu, *Adv. Energy Mater.* 2020, **10**, 1903664.

3. Y. Xiao, D. Su, X. Wang, S. Wu, L. Zhou, Y. Shi, S. Fang, H.-M. Cheng and F. Li, *Adv. Energy Mater.*, 2018, **8**, 1800930.

4. Y. Wang, Y. Lu, W. Zhan, Z. Xie, Q. Kuang and L. Zheng, *J. Mater. Chem. A*, 2015, **3**, 12796−12803.

5. Y. Shen, Y. Wang, Y. Miao, M. Yang, X. Zhao and X. Shen, *Adv. Mater.*, 2020, **32**, e1905524.

6. J. Kim, W. Cho, J. W. Park, C. Kim, M. Kim and H. Song, *J. Am. Chem. Soc.* 2019, **141**, 6986−6994.

7. W. He, I. Liberman, I. Rozenberg, R. Ifraemov and I. Hod, *Angew. Chem. Int. Ed.*, 2020, **59**, 8262−8269.

8. T. Shinagawa, G. O. Larrazábal, A. J. Martín, F. Krumeich and J. Pérez-Ramírez, *ACS Catal.*, 2018, **8**, 837−844.

9. Y. Deng, Y. Huang, D. Ren, A. D. Handoko, Z. W. Seh, P. Hirunsit and B. S. Yeo, *ACS Appl. Mater. Inter.* 2018, **10**, 28572−28581.

10. Y. Huang, Y. Deng, A. D. Handoko, G. K. L. Goh and B. S. Yeo, *ChemSusChem*, 2018, **11**, 320−326.

11. J. Li, J. Jiao, H. Zhang, P. Zhu, H. Ma, C. Chen, H. Xiao and Q. Lu, *ACS Sustainable Chem. Eng.*, 2020, **8**, 4975−4982.

12. A. Zhang, Y. Liang, H. Li, S. Wang, Q. Chang, K. Peng, Z. Geng and J. Zeng, *Nano Lett.,* 2021, **21**, 7789−7795.

13. Li, F., L. Chen, G. P. Knowles, D. R. MacFarlane and J. Zhang, *Angew. Chem. Int. Ed.*, 2017, **56**, 505−509.

14. P. Deng, F. Yang, Z. Wang, S. Chen, Y. Zhou, S. Zaman and B. Y. Xia, *Angew. Chem. Int. Ed.* 2020, **59**, 10807−10813.

15. D. Yao, C. Tang, A. Vasileff, X. Zhi, Y. Jiao and S. Z. Qiao, *Angew. Chem. Int. Ed.*, 2021, **60**, 18178−18184.

16. M. Fan, S. Prabhudev, S. Garbarino, J. Qiao, G. A. Botton, D. A. Harrington, A. C. Tavares and D. Guay, *Appl. Catal. B: Environ.*, 2020, **274**, 119031.

17. W. Ma, J. Bu, Z. Liu, C. Yan, Y. Yao, N. Chang, H. Zhang, T. Wang and J. Zhang, *Adv. Fun. Mater.*, 2020, **31**, 2006704.